

**Study of  $X(3915) \rightarrow J/\psi\omega$  in two-photon collisions**

J. P. Lees,<sup>1</sup> V. Poireau,<sup>1</sup> V. Tisserand,<sup>1</sup> J. Garra Tico,<sup>2</sup> E. Grauges,<sup>2</sup> A. Palano,<sup>3a,3b</sup> G. Eigen,<sup>4</sup> B. Stugu,<sup>4</sup> D. N. Brown,<sup>5</sup> L. T. Kerth,<sup>5</sup> Yu. G. Kolomensky,<sup>5</sup> G. Lynch,<sup>5</sup> H. Koch,<sup>6</sup> T. Schroeder,<sup>6</sup> D. J. Asgeirsson,<sup>7</sup> C. Hearty,<sup>7</sup> T. S. Mattison,<sup>7</sup> J. A. McKenna,<sup>7</sup> R. Y. So,<sup>7</sup> A. Khan,<sup>8</sup> V. E. Blinov,<sup>9</sup> A. R. Buzykaev,<sup>9</sup> V. P. Druzhinin,<sup>9</sup> V. B. Golubev,<sup>9</sup> E. A. Kravchenko,<sup>9</sup> A. P. Onuchin,<sup>9</sup> S. I. Serednyakov,<sup>9</sup> Yu. I. Skovpen,<sup>9</sup> E. P. Solodov,<sup>9</sup> K. Yu. Todyshev,<sup>9</sup> A. N. Yushkov,<sup>9</sup> M. Bondioli,<sup>10</sup> D. Kirkby,<sup>10</sup> A. J. Lankford,<sup>10</sup> M. Mandelkern,<sup>10</sup> H. Atmacan,<sup>11</sup> J. W. Gary,<sup>11</sup> F. Liu,<sup>11</sup> O. Long,<sup>11</sup> G. M. Vitug,<sup>11</sup> C. Campagnari,<sup>12</sup> T. M. Hong,<sup>12</sup> D. Kovalskyi,<sup>12</sup> J. D. Richman,<sup>12</sup> C. A. West,<sup>12</sup> A. M. Eisner,<sup>13</sup> J. Kroseberg,<sup>13</sup> W. S. Lockman,<sup>13</sup> A. J. Martinez,<sup>13</sup> B. A. Schumm,<sup>13</sup> A. Seiden,<sup>13</sup> D. S. Chao,<sup>14</sup> C. H. Cheng,<sup>14</sup> B. Echenard,<sup>14</sup> K. T. Flood,<sup>14</sup> D. G. Hitlin,<sup>14</sup> P. Ongmongkolkul,<sup>14</sup> F. C. Porter,<sup>14</sup> A. Y. Rakin,<sup>14</sup> R. Andreassen,<sup>15</sup> Z. Huard,<sup>15</sup> B. T. Meadows,<sup>15</sup> M. D. Sokoloff,<sup>15</sup> L. Sun,<sup>15</sup> P. C. Bloom,<sup>16</sup> W. T. Ford,<sup>16</sup> A. Gaz,<sup>16</sup> U. Nauenberg,<sup>16</sup> J. G. Smith,<sup>16</sup> S. R. Wagner,<sup>16</sup> R. Ayad,<sup>17,\*</sup> W. H. Toki,<sup>17</sup> B. Spaan,<sup>18</sup> K. R. Schubert,<sup>19</sup> R. Schwierz,<sup>19</sup> D. Bernard,<sup>20</sup> M. Verderi,<sup>20</sup> P. J. Clark,<sup>21</sup> S. Playfer,<sup>21</sup> D. Bettoni,<sup>22a</sup> C. Bozzi,<sup>22a</sup> R. Calabrese,<sup>22a,22b</sup> G. Cibinetto,<sup>22a,22b</sup> E. Fioravanti,<sup>22a,22b</sup> I. Garzia,<sup>22a,22b</sup> E. Luppi,<sup>22a,22b</sup> M. Munerato,<sup>22a,22b</sup> L. Piemontese,<sup>22a</sup> V. Santoro,<sup>22a</sup> R. Baldini-Ferrolì,<sup>23</sup> A. Calcaterra,<sup>23</sup> R. de Sangro,<sup>23</sup> G. Finocchiaro,<sup>23</sup> P. Patteri,<sup>23</sup> I. M. Peruzzi,<sup>23,†</sup> M. Piccolo,<sup>23</sup> M. Rama,<sup>23</sup> A. Zallo,<sup>23</sup> R. Contri,<sup>24a,24b</sup> E. Guido,<sup>24a,24b</sup> M. Lo Vetere,<sup>24a,24b</sup> M. R. Monge,<sup>24a,24b</sup> S. Passaggio,<sup>24a</sup> C. Patrignani,<sup>24a,24b</sup> E. Robutti,<sup>24a</sup> B. Bhuyan,<sup>25</sup> V. Prasad,<sup>25</sup> C. L. Lee,<sup>26</sup> M. Morii,<sup>26</sup> A. J. Edwards,<sup>27</sup> A. Adametz,<sup>28</sup> U. Uwer,<sup>28</sup> H. M. Lacker,<sup>29</sup> T. Lueck,<sup>29</sup> P. D. Dauncey,<sup>30</sup> U. Mallik,<sup>31</sup> C. Chen,<sup>32</sup> J. Cochran,<sup>32</sup> W. T. Meyer,<sup>32</sup> S. Prell,<sup>32</sup> A. E. Rubin,<sup>32</sup> A. V. Gritsan,<sup>33</sup> Z. J. Guo,<sup>33</sup> N. Arnaud,<sup>34</sup> M. Davier,<sup>34</sup> D. Derkach,<sup>34</sup> G. Grosdidier,<sup>34</sup> F. Le Diberder,<sup>34</sup> A. M. Lutz,<sup>34</sup> B. Malaescu,<sup>34</sup> P. Roudeau,<sup>34</sup> M. H. Schune,<sup>34</sup> A. Stocchi,<sup>34</sup> G. Wormser,<sup>34</sup> D. J. Lange,<sup>35</sup> D. M. Wright,<sup>35</sup> C. A. Chavez,<sup>36</sup> J. P. Coleman,<sup>36</sup> J. R. Fry,<sup>36</sup> E. Gabathuler,<sup>36</sup> D. E. Hutchcroft,<sup>36</sup> D. J. Payne,<sup>36</sup> C. Touramanis,<sup>36</sup> A. J. Bevan,<sup>37</sup> F. Di Lodovico,<sup>37</sup> R. Sacco,<sup>37</sup> M. Sigamani,<sup>37</sup> G. Cowan,<sup>38</sup> D. N. Brown,<sup>39</sup> C. L. Davis,<sup>39</sup> A. G. Denig,<sup>40</sup> M. Fritsch,<sup>40</sup> W. Gradl,<sup>40</sup> K. Griessinger,<sup>40</sup> A. Hafner,<sup>40</sup> E. Prencipe,<sup>40</sup> R. J. Barlow,<sup>41,‡</sup> G. Jackson,<sup>41</sup> G. D. Lafferty,<sup>41</sup> E. Behn,<sup>42</sup> R. Cenci,<sup>42</sup> B. Hamilton,<sup>42</sup> A. Jawahery,<sup>42</sup> D. A. Roberts,<sup>42</sup> C. Dallapiccola,<sup>43</sup> R. Cowan,<sup>44</sup> D. Dujmic,<sup>44</sup> G. Sciolla,<sup>44</sup> R. Cheaib,<sup>45</sup> D. Lindemann,<sup>45</sup> P. M. Patel,<sup>45,§</sup> S. H. Robertson,<sup>45</sup> P. Biassoni,<sup>46a,46b</sup> N. Neri,<sup>46a</sup> F. Palombo,<sup>46a,46b</sup> S. Stracka,<sup>46a,46b</sup> L. Cremaldi,<sup>47</sup> R. Godang,<sup>47,||</sup> R. Kroeger,<sup>47</sup> P. Sonnek,<sup>47</sup> D. J. Summers,<sup>47</sup> X. Nguyen,<sup>48</sup> M. Simard,<sup>48</sup> P. Taras,<sup>48</sup> G. De Nardo,<sup>49a,49b</sup> D. Monorchio,<sup>49a,49b</sup> G. Onorato,<sup>49a,49b</sup> C. Sciacca,<sup>49a,49b</sup> M. Martinelli,<sup>50</sup> G. Raven,<sup>50</sup> C. P. Jessop,<sup>51</sup> J. M. LoSecco,<sup>51</sup> W. F. Wang,<sup>51</sup> K. Honscheid,<sup>52</sup> R. Kass,<sup>52</sup> J. Brau,<sup>53</sup> R. Frey,<sup>53</sup> N. B. Sinev,<sup>53</sup> D. Strom,<sup>53</sup> E. Torrence,<sup>53</sup> E. Feltresi,<sup>54a,54b</sup> N. Gagliardi,<sup>54a,54b</sup> M. Margoni,<sup>54a,54b</sup> M. Morandin,<sup>54a</sup> M. Posocco,<sup>54a</sup> M. Rotondo,<sup>54a</sup> G. Simi,<sup>54a</sup> F. Simonetto,<sup>54a,54b</sup> R. Stroili,<sup>54a,54b</sup> S. Akar,<sup>55</sup> E. Ben-Haim,<sup>55</sup> M. Bomben,<sup>55</sup> G. R. Bonneaud,<sup>55</sup> H. Briand,<sup>55</sup> G. Calderini,<sup>55</sup> J. Chauveau,<sup>55</sup> O. Hamon,<sup>55</sup> Ph. Leruste,<sup>55</sup> G. Marchiori,<sup>55</sup> J. Ocariz,<sup>55</sup> S. Sitt,<sup>55</sup> M. Biasini,<sup>56a,56a</sup> E. Manoni,<sup>56a,56a</sup> S. Pacetti,<sup>56a,56a</sup> A. Rossi,<sup>56a,56a</sup> C. Angelini,<sup>57a,57b</sup> G. Batignani,<sup>57a,57b</sup> S. Bettarini,<sup>57a,57b</sup> M. Carpinelli,<sup>57a,57b,¶</sup> G. Casarosa,<sup>57a,57b</sup> A. Cervelli,<sup>57a,57b</sup> F. Forti,<sup>57a,57b</sup> M. A. Giorgi,<sup>57a,57b</sup> A. Lusiani,<sup>57a,57c</sup> B. Oberhof,<sup>57a,57b</sup> E. Paoloni,<sup>57a,57b</sup> A. Perez,<sup>57a</sup> G. Rizzo,<sup>57a,57b</sup> J. J. Walsh,<sup>57a</sup> D. Lopes Pegna,<sup>58</sup> J. Olsen,<sup>58</sup> A. J. S. Smith,<sup>58</sup> A. V. Telnov,<sup>58</sup> F. Anulli,<sup>59a</sup> R. Faccini,<sup>59a,59b</sup> F. Ferrarotto,<sup>59a</sup> F. Ferroni,<sup>59a,59b</sup> M. Gaspero,<sup>59a,59b</sup> L. Li Gioi,<sup>59a</sup> M. A. Mazzoni,<sup>59a</sup> G. Piredda,<sup>59a</sup> C. Büniger,<sup>60</sup> O. Grünberg,<sup>60</sup> T. Hartmann,<sup>60</sup> T. Leddig,<sup>60</sup> C. Voß,<sup>60</sup> R. Waldi,<sup>60</sup> T. Adye,<sup>61</sup> E. O. Olaiya,<sup>61</sup> F. F. Wilson,<sup>61</sup> S. Emery,<sup>62</sup> G. Hamel de Monchenault,<sup>62</sup> G. Vasseur,<sup>62</sup> Ch. Yèche,<sup>62</sup> D. Aston,<sup>63</sup> D. J. Bard,<sup>63</sup> R. Bartoldus,<sup>63</sup> J. F. Benitez,<sup>63</sup> C. Cartaro,<sup>63</sup> M. R. Convery,<sup>63</sup> J. Dorfan,<sup>63</sup> G. P. Dubois-Felsmann,<sup>63</sup> W. Dunwoodie,<sup>63</sup> M. Ebert,<sup>63</sup> R. C. Field,<sup>63</sup> M. Franco Sevilla,<sup>63</sup> B. G. Fulsom,<sup>63</sup> A. M. Gabareen,<sup>63</sup> M. T. Graham,<sup>63</sup> P. Grenier,<sup>63</sup> C. Hast,<sup>63</sup> W. R. Innes,<sup>63</sup> M. H. Kelsey,<sup>63</sup> P. Kim,<sup>63</sup> M. L. Kocian,<sup>63</sup> D. W. G. S. Leith,<sup>63</sup> P. Lewis,<sup>63</sup> B. Lindquist,<sup>63</sup> S. Luitz,<sup>63</sup> V. Luth,<sup>63</sup> H. L. Lynch,<sup>63</sup> D. B. MacFarlane,<sup>63</sup> D. R. Muller,<sup>63</sup> H. Neal,<sup>63</sup> S. Nelson,<sup>63</sup> M. Perl,<sup>63</sup> T. Pulliam,<sup>63</sup> B. N. Ratcliff,<sup>63</sup> A. Roodman,<sup>63</sup> A. A. Salnikov,<sup>63</sup> R. H. Schindler,<sup>63</sup> A. Snyder,<sup>63</sup> D. Su,<sup>63</sup> M. K. Sullivan,<sup>63</sup> J. Va'vra,<sup>63</sup> A. P. Wagner,<sup>63</sup> W. J. Wisniewski,<sup>63</sup> M. Wittgen,<sup>63</sup> D. H. Wright,<sup>63</sup> H. W. Wulsin,<sup>63</sup> C. C. Young,<sup>63</sup> V. Ziegler,<sup>63</sup> W. Park,<sup>64</sup> M. V. Purohit,<sup>64</sup> R. M. White,<sup>64</sup> J. R. Wilson,<sup>64</sup> A. Randle-Conde,<sup>65</sup> S. J. Sekula,<sup>65</sup> M. Bellis,<sup>66</sup> P. R. Burchat,<sup>66</sup> T. S. Miyashita,<sup>66</sup> E. M. T. Puccio,<sup>66</sup> M. S. Alam,<sup>67</sup> J. A. Ernst,<sup>67</sup> R. Gorodeisky,<sup>68</sup> N. Guttman,<sup>68</sup> D. R. Peimer,<sup>68</sup> A. Soffer,<sup>68</sup> P. Lund,<sup>69</sup> S. M. Spanier,<sup>69</sup> J. L. Ritchie,<sup>70</sup> A. M. Ruland,<sup>70</sup> R. F. Schwitters,<sup>70</sup> B. C. Wray,<sup>70</sup> J. M. Izen,<sup>71</sup> X. C. Lou,<sup>71</sup> F. Bianchi,<sup>72a,72b</sup> D. Gamba,<sup>72a,72b</sup> S. Zambito,<sup>72a,72b</sup> L. Lancieri,<sup>73a,73b</sup> L. Vitale,<sup>73a,73b</sup> F. Martinez-Vidal,<sup>74</sup> A. Oyanguren,<sup>74</sup> P. Villanueva-Perez,<sup>74</sup> H. Ahmed,<sup>75</sup> J. Albert,<sup>75</sup> Sw. Banerjee,<sup>75</sup> F. U. Bernlochner,<sup>75</sup> H. H. F. Choi,<sup>75</sup> G. J. King,<sup>75</sup> R. Kowalewski,<sup>75</sup> M. J. Lewczuk,<sup>75</sup> I. M. Nugent,<sup>75</sup> J. M. Roney,<sup>75</sup> R. J. Sobie,<sup>75</sup> N. Tasneem,<sup>75</sup> T. J. Gershon,<sup>76</sup> P. F. Harrison,<sup>76</sup> T. E. Latham,<sup>76</sup> H. R. Band,<sup>77</sup> S. Dasu,<sup>77</sup> Y. Pan,<sup>77</sup> R. Prepost,<sup>77</sup> and S. L. Wu<sup>77</sup>

## (BABAR Collaboration)

- <sup>1</sup>Laboratoire d'Annecy-le-Vieux de Physique des Particules (LAPP), Université de Savoie, CNRS/IN2P3, F-74941 Annecy-Le-Vieux, France
- <sup>2</sup>Universitat de Barcelona, Facultat de Física, Departament ECM, E-08028 Barcelona, Spain
- <sup>3a</sup>INFN Sezione di Bari, I-70126 Bari, Italy
- <sup>3b</sup>Dipartimento di Fisica, Università di Bari, I-70126 Bari, Italy
- <sup>4</sup>University of Bergen, Institute of Physics, N-5007 Bergen, Norway
- <sup>5</sup>Lawrence Berkeley National Laboratory and University of California, Berkeley, California 94720, USA
- <sup>6</sup>Ruhr Universität Bochum, Institut für Experimentalphysik 1, D-44780 Bochum, Germany
- <sup>7</sup>University of British Columbia, Vancouver, British Columbia, Canada V6T 1Z1
- <sup>8</sup>Brunel University, Uxbridge, Middlesex UB8 3PH, United Kingdom
- <sup>9</sup>Budker Institute of Nuclear Physics, Novosibirsk 630090, Russia
- <sup>10</sup>University of California at Irvine, Irvine, California 92697, USA
- <sup>11</sup>University of California at Riverside, Riverside, California 92521, USA
- <sup>12</sup>University of California at Santa Barbara, Santa Barbara, California 93106, USA
- <sup>13</sup>University of California at Santa Cruz, Institute for Particle Physics, Santa Cruz, California 95064, USA
- <sup>14</sup>California Institute of Technology, Pasadena, California 91125, USA
- <sup>15</sup>University of Cincinnati, Cincinnati, Ohio 45221, USA
- <sup>16</sup>University of Colorado, Boulder, Colorado 80309, USA
- <sup>17</sup>Colorado State University, Fort Collins, Colorado 80523, USA
- <sup>18</sup>Technische Universität Dortmund, Fakultät Physik, D-44221 Dortmund, Germany
- <sup>19</sup>Technische Universität Dresden, Institut für Kern- und Teilchenphysik, D-01062 Dresden, Germany
- <sup>20</sup>Laboratoire Leprince-Ringuet, Ecole Polytechnique, CNRS/IN2P3, F-91128 Palaiseau, France
- <sup>21</sup>University of Edinburgh, Edinburgh EH9 3JZ, United Kingdom
- <sup>22a</sup>INFN Sezione di Ferrara, I-44100 Ferrara, Italy
- <sup>22b</sup>Dipartimento di Fisica, Università di Ferrara, I-44100 Ferrara, Italy
- <sup>23</sup>INFN Laboratori Nazionali di Frascati, I-00044 Frascati, Italy
- <sup>24a</sup>INFN Sezione di Genova, I-16146 Genova, Italy
- <sup>24b</sup>Dipartimento di Fisica, Università di Genova, I-16146 Genova, Italy
- <sup>25</sup>Indian Institute of Technology Guwahati, Guwahati, Assam, 781 039, India
- <sup>26</sup>Harvard University, Cambridge, Massachusetts 02138, USA
- <sup>27</sup>Harvey Mudd College, Claremont, California 91711, USA
- <sup>28</sup>Universität Heidelberg, Physikalisches Institut, Philosophenweg 12, D-69120 Heidelberg, Germany
- <sup>29</sup>Humboldt-Universität zu Berlin, Institut für Physik, Newtonstrasse 15, D-12489 Berlin, Germany
- <sup>30</sup>Imperial College London, London, SW7 2AZ, United Kingdom
- <sup>31</sup>University of Iowa, Iowa City, Iowa 52242, USA
- <sup>32</sup>Iowa State University, Ames, Iowa 50011-3160, USA
- <sup>33</sup>Johns Hopkins University, Baltimore, Maryland 21218, USA
- <sup>34</sup>Laboratoire de l'Accélérateur Linéaire, IN2P3/CNRS et Université Paris-Sud 11, Centre Scientifique d'Orsay, B.P. 34, F-91898 Orsay Cedex, France
- <sup>35</sup>Lawrence Livermore National Laboratory, Livermore, California 94550, USA
- <sup>36</sup>University of Liverpool, Liverpool L69 7ZE, United Kingdom
- <sup>37</sup>Queen Mary, University of London, London, E1 4NS, United Kingdom
- <sup>38</sup>University of London, Royal Holloway and Bedford New College, Egham, Surrey TW20 0EX, United Kingdom
- <sup>39</sup>University of Louisville, Louisville, Kentucky 40292, USA
- <sup>40</sup>Johannes Gutenberg-Universität Mainz, Institut für Kernphysik, D-55099 Mainz, Germany
- <sup>41</sup>University of Manchester, Manchester M13 9PL, United Kingdom
- <sup>42</sup>University of Maryland, College Park, Maryland 20742, USA
- <sup>43</sup>University of Massachusetts, Amherst, Massachusetts 01003, USA
- <sup>44</sup>Massachusetts Institute of Technology, Laboratory for Nuclear Science, Cambridge, Massachusetts 02139, USA
- <sup>45</sup>McGill University, Montréal, Québec, Canada H3A 2T8
- <sup>46a</sup>INFN Sezione di Milano, I-20133 Milano, Italy
- <sup>46b</sup>Dipartimento di Fisica, Università di Milano, I-20133 Milano, Italy
- <sup>47</sup>University of Mississippi, University, Mississippi 38677, USA
- <sup>48</sup>Université de Montréal, Physique des Particules, Montréal, Québec, Canada H3C 3J7
- <sup>49a</sup>INFN Sezione di Napoli, I-80126 Napoli, Italy
- <sup>49b</sup>Dipartimento di Scienze Fisiche, Università di Napoli Federico II, I-80126 Napoli, Italy
- <sup>50</sup>NIKHEF, National Institute for Nuclear Physics and High Energy Physics, NL-1009 DB Amsterdam, Netherlands

- <sup>51</sup>University of Notre Dame, Notre Dame, Indiana 46556, USA  
<sup>52</sup>Ohio State University, Columbus, Ohio 43210, USA  
<sup>53</sup>University of Oregon, Eugene, Oregon 97403, USA  
<sup>54a</sup>INFN Sezione di Padova, I-35131 Padova, Italy  
<sup>54b</sup>Dipartimento di Fisica, Università di Padova, I-35131 Padova, Italy  
<sup>55</sup>Laboratoire de Physique Nucléaire et de Hautes Energies, IN2P3/CNRS, Université Pierre et Marie Curie-Paris6, Université Denis Diderot-Paris7, F-75252 Paris, France  
<sup>56a</sup>INFN Sezione di Perugia, I-06100 Perugia, Italy  
<sup>56a</sup>Dipartimento di Fisica, Università di Perugia, I-06100 Perugia, Italy  
<sup>57a</sup>INFN Sezione di Pisa, I-56127 Pisa, Italy  
<sup>57b</sup>Dipartimento di Fisica, Università di Pisa, I-56127 Pisa, Italy  
<sup>57c</sup>Scuola Normale Superiore di Pisa, I-56127 Pisa, Italy  
<sup>58</sup>Princeton University, Princeton, New Jersey 08544, USA  
<sup>59a</sup>INFN Sezione di Roma, I-00185 Roma, Italy  
<sup>59b</sup>Dipartimento di Fisica, Università di Roma La Sapienza, I-00185 Roma, Italy  
<sup>60</sup>Universität Rostock, D-18051 Rostock, Germany  
<sup>61</sup>Rutherford Appleton Laboratory, Chilton, Didcot, Oxon, OX11 0QX, United Kingdom  
<sup>62</sup>CEA, Irfu, SPP, Centre de Saclay, F-91191 Gif-sur-Yvette, France  
<sup>63</sup>SLAC National Accelerator Laboratory, Stanford, California 94309 USA  
<sup>64</sup>University of South Carolina, Columbia, South Carolina 29208, USA  
<sup>65</sup>Southern Methodist University, Dallas, Texas 75275, USA  
<sup>66</sup>Stanford University, Stanford, California 94305-4060, USA  
<sup>67</sup>State University of New York, Albany, New York 12222, USA  
<sup>68</sup>Tel Aviv University, School of Physics and Astronomy, Tel Aviv, 69978, Israel  
<sup>69</sup>University of Tennessee, Knoxville, Tennessee 37996, USA  
<sup>70</sup>University of Texas at Austin, Austin, Texas 78712, USA  
<sup>71</sup>University of Texas at Dallas, Richardson, Texas 75083, USA  
<sup>72a</sup>INFN Sezione di Torino, I-10125 Torino, Italy  
<sup>72b</sup>Dipartimento di Fisica Sperimentale, Università di Torino, I-10125 Torino, Italy  
<sup>73a</sup>INFN Sezione di Trieste, I-34127 Trieste, Italy  
<sup>73b</sup>Dipartimento di Fisica, Università di Trieste, I-34127 Trieste, Italy  
<sup>74</sup>IFIC, Universitat de Valencia-CSIC, E-46071 Valencia, Spain  
<sup>75</sup>University of Victoria, Victoria, British Columbia, Canada V8W 3P6  
<sup>76</sup>Department of Physics, University of Warwick, Coventry CV4 7AL, United Kingdom  
<sup>77</sup>University of Wisconsin, Madison, Wisconsin 53706, USA  
(Received 12 July 2012; published 1 October 2012)

We study the process  $\gamma\gamma \rightarrow J/\psi \omega$  using a data sample of  $519.2 \text{ fb}^{-1}$  recorded by the *BABAR* detector at SLAC at the PEP-II asymmetric-energy  $e^+e^-$  collider at center-of-mass energies near the  $Y(nS)$  ( $n = 2, 3, 4$ ) resonances. We confirm the existence of the charmoniumlike resonance  $X(3915)$  decaying to  $J/\psi \omega$  with a significance of 7.6 standard deviations, including systematic uncertainties, and measure its mass  $(3919.4 \pm 2.2 \pm 1.6) \text{ MeV}/c^2$  and width  $(13 \pm 6 \pm 3) \text{ MeV}$ , where the first uncertainty is statistical and the second systematic. A spin-parity analysis supports the assignment  $J^P = 0^+$  and therefore the identification of the signal as due to the  $\chi_{c0}(2P)$  resonance. In this hypothesis we determine the product between the two-photon width and the final state branching fraction to be  $(52 \pm 10 \pm 3) \text{ eV}$ .

DOI: [10.1103/PhysRevD.86.072002](https://doi.org/10.1103/PhysRevD.86.072002)

PACS numbers: 13.25.Gv, 14.40.Pq, 14.40.Rt

## I. INTRODUCTION

In the last several years many new charmoniumlike states have been observed in the mass region between 3.7 and 5.0  $\text{GeV}/c^2$ , above the  $D\bar{D}$  threshold, with properties that disfavor their interpretation as conventional charmonium mesons [1–5]. The  $X(3915)$  resonance, decaying to the  $J/\psi \omega$  final state, was first observed by the Belle Collaboration in two-photon collisions [6]. Another resonance, dubbed  $Y(3940)$ , has been observed in the  $B \rightarrow J/\psi \omega K$  process [4,5,7]. The mass measurement for the  $Y(3940)$  [4,5,7] is consistent with that of the  $X(3915)$  [6].

\*Present address: the University of Tabuk, Tabuk 71491, Saudi Arabia.

†Also at Università di Perugia, Dipartimento di Fisica, Perugia, Italy.

‡Present address: the University of Huddersfield, Huddersfield HD1 3DH, United Kingdom.

§Deceased.

||Present address: University of South Alabama, Mobile, AL 36688, USA.

¶Also at Università di Sassari, Sassari, Italy.

Thus, the same particle, with a mass of about  $3915 \text{ MeV}/c^2$ , may have been observed in two distinct production processes. The  $Z(3930)$  resonance has been discovered in the  $\gamma\gamma \rightarrow D\bar{D}$  process [2,3]. Its interpretation as the  $\chi_{c2}(2P)$ , the first radial excitation of the  ${}^3P_2$  charmonium ground state, is commonly accepted [8]. Interpretation of the  $X(3915)$  as the  $\chi_{c0}(2P)$  [9] or  $\chi_{c2}(2P)$  state [10] has been suggested. The latter implies that the  $X(3915)$  and  $Z(3930)$  are the same particle, observed in different decay modes. However, the product of the two-photon width times the decay branching fraction  $\mathcal{B}$  for the  $X(3915)$  reported by Belle [6] is unexpectedly large compared to other excited  $c\bar{c}$  states [8]. Interpretation of the  $X(3915)$  in the framework of molecular models has also been proposed [11].

Despite the many measurements available [8], the nature of the  $X(3872)$  state, which was first observed by Belle [12], is still unclear [13]. The observation of its decay into  $\gamma J/\psi$  [14] ensures that this particle has positive  $C$  parity. The spin analysis performed by CDF on the decay  $X(3872) \rightarrow J/\psi \pi^+ \pi^-$  concludes that only  $J^P = 1^+$  and  $J^P = 2^-$  are consistent with data [15]. Similarly, a recent spin analysis performed by Belle [16] concludes that  $J^P = 1^+$  describes the data as does  $J^P = 2^-$  with one free parameter. An analysis of the  $\pi^+ \pi^- \pi^0$  mass distribution in the  $X(3872) \rightarrow J/\psi \omega$  decay performed by BABAR favors the spin-parity assignment  $J^P = 2^-$  [7], but a  $J^P = 1^+$  spin assignment is not ruled out. If  $J^P = 2^-$ , the production of the  $X(3872)$  in two-photon collisions would be allowed.

In this paper we search for the  $X(3915)$  and  $X(3872)$  resonances in the two-photon process  $e^+ e^- \rightarrow e^+ e^- \gamma\gamma \rightarrow e^+ e^- J/\psi \omega$ , where  $J/\psi \rightarrow \ell^+ \ell^-$  ( $\ell = e$  or  $\mu$ ) and  $\omega \rightarrow \pi^+ \pi^- \pi^0$ . Two-photon events where the interacting photons are not quasireal are strongly suppressed in this analysis by the selection criteria described below. This implies that the allowed  $J^{PC}$  values of any produced resonances are  $0^{\pm+}, 2^{\pm+}, 4^{\pm+}, \dots; 3^{++}, 5^{++}, \dots$  [17]. Angular momentum conservation, parity conservation, and charge conjugation invariance then imply that these quantum numbers also apply to the final state.

This paper is organized as follows. In Sec. II we give a brief description of the BABAR detector. Section III is devoted to the event reconstruction and data selection. In Sec. IV we present the study of the  $J/\psi \omega$  system while in Sec. V we perform an angular analysis of  $X(3915)$ . The study of systematic uncertainties is described in Sec. VI. In Sec. VII we summarize the results.

## II. THE BABAR DETECTOR

The results presented here are based on data collected with the BABAR detector at the PEP-II asymmetric-energy  $e^+ e^-$  collider located at the SLAC National Accelerator Laboratory and correspond to an integrated luminosity of  $519.2 \text{ fb}^{-1}$  recorded at center-of-mass energies near the

$\Upsilon(nS)$  ( $n = 2, 3, 4$ ) resonances. The BABAR detector is described in detail elsewhere [18]. Charged particles are detected, and their momenta are measured, by a five-layer double-sided microstrip detector and a 40-layer drift chamber, both operating in the 1.5 T magnetic field of a superconducting solenoid. Photons and electrons are identified in a CsI(Tl) crystal electromagnetic calorimeter. Charged-particle identification is provided by the specific energy loss in the tracking devices and by an internally reflecting, ring-imaging Cherenkov detector. Muons and neutral  $K_L^0$  mesons are detected in the instrumented flux return of the magnet. Monte Carlo (MC) simulated events [19], with sample sizes more than 10 times larger than the corresponding data samples, are used to evaluate the signal efficiency and determine background features. Two-photon events are simulated using the GamGam MC generator [3].

## III. EVENT RECONSTRUCTION AND DATA SELECTION

In this analysis we select events in which the  $e^+$  and  $e^-$  beam particles are scattered at small angles and remain undetected. In the  $\gamma\gamma \rightarrow J/\psi \omega$  process, the  $J/\psi$  is reconstructed in the  $\ell^+ \ell^-$  final state, with  $\ell = e$  or  $\mu$ , while the  $\omega$  is reconstructed in its dominant  $\pi^+ \pi^- \pi^0$  decay mode. We only consider events where the number of well-measured charged tracks having a transverse momentum greater than  $0.1 \text{ GeV}/c$  is exactly equal to four.

Neutral pions are reconstructed through the  $\pi^0 \rightarrow \gamma\gamma$  decay. We require the invariant mass of a  $\pi^0$  candidate to be in the range (115–150)  $\text{MeV}/c^2$ , and its energy in the laboratory system to be larger than 200 MeV. The energy in the laboratory frame of the most energetic photon from  $\pi^0$  decay is required to be smaller than 1.4 GeV in order to suppress  $\pi^0$ 's not originating from an  $\omega$  decay. We require the energy of the least energetic photon from  $\pi^0$  decay to be in the range (0.04–0.60) GeV, and  $|\cos \mathcal{H}_{\pi^0}| < 0.9$ , where  $\mathcal{H}_{\pi^0}$  is the angle between the signal  $\pi^0$  flight direction in the laboratory frame and the direction of one of its daughters in its rest frame. These requirements are optimized by maximizing  $S/\sqrt{S+B}$ , where  $S$  is the number of MC signal events with a well-reconstructed  $\pi^0$ , and  $B$  is the number of MC signal events where the  $\pi^0$  is misreconstructed. The  $\omega$  is reconstructed by combining two oppositely charged tracks identified as pions with one  $\pi^0$ . The  $\omega$  signal region is defined as  $740 < m(\pi^+ \pi^- \pi^0) < 820 \text{ MeV}/c^2$ . The  $J/\psi$  is reconstructed by combining two tracks that are identified as oppositely charged muons or electrons. The measured electron energy is corrected to account for energy deposits in the electromagnetic calorimeter consistent with bremsstrahlung radiation. We require the vertex fit probability of the two leptons to be larger than 0.1%. The  $J/\psi$  signal region is defined as  $2.95 < m(e^+ e^-) < 3.14 \text{ GeV}/c^2$  for  $e^+ e^-$  and  $3.05 < m(\mu^+ \mu^-) < 3.14 \text{ GeV}/c^2$  for  $\mu^+ \mu^-$  events. An event with a  $J/\psi \omega$  candidate is constructed by fitting the  $J/\psi$

and  $\omega$  candidates to a common vertex. The  $\pi^0$  mass is constrained to its nominal value [8] in this fit. Charged particles are required to originate from the interaction region. We require the vertex fit probability of the charmonium candidate to be larger than 0.1%.

Background arises mainly from random combinations of particles from  $e^+e^-$  annihilation, other two-photon collisions, and initial-state radiation (ISR) processes. We discriminate against  $J/\psi \pi^+ \pi^- \pi^0$  events produced via ISR by requiring  $M_{\text{miss}}^2 \equiv (p_{e^+e^-} - p_{\text{rec}})^2 > 2 (\text{GeV}/c^2)^2$ , where  $p_{e^+e^-}$  ( $p_{\text{rec}}$ ) is the four-momentum of the initial state ( $J/\psi \omega$  final state). We define  $p_T$  as the transverse momentum, in the  $e^+e^-$  rest frame, of the  $J/\psi \omega$  candidate with respect to the beam axis. Well-reconstructed two-photon events are expected to have a low transverse momentum  $p_T$  and a small amount of electromagnetic calorimeter energy  $E_{\text{extra}}$ , i.e., energy not associated with the final state particles. We require  $p_T < 0.2 \text{ GeV}/c$  and  $E_{\text{extra}} < 0.3 \text{ GeV}$ . Events originating from residual ISR  $\psi(2S) \rightarrow J/\psi \pi^+ \pi^-$  decays may create fake structures in the  $J/\psi \omega$  mass spectrum. We therefore remove events in the mass window  $3.675 < m(J/\psi \pi^+ \pi^-) < 3.700 \text{ GeV}/c^2$ , where  $m(J/\psi \pi^+ \pi^-) = m(\ell^+ \ell^- \pi^+ \pi^-) - m(\ell^+ \ell^-) + m(J/\psi)^{\text{PDG}}$  and  $m(J/\psi)^{\text{PDG}}$  is the nominal  $J/\psi$  mass [8].

The  $J/\psi \omega$  signal region is defined as the intersection of the  $J/\psi$  and  $\omega$  signal regions defined above. In about 10% of the events we find more than one candidate, and we select the one having the lowest  $p_T$  value. We obtain 95 events in the  $J/\psi \omega$  signal region.

#### IV. STUDY OF THE $J/\psi \omega$ SYSTEM

Figure 1 shows the  $p_T$  distribution for the selected candidates, obtained by applying the above requirements with the exception of that on  $p_T$ . The distribution is fitted with the signal  $p_T$  shape obtained from MC simulation plus

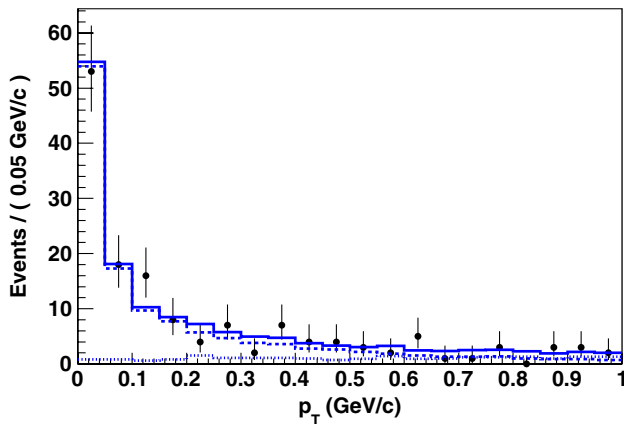


FIG. 1 (color online). The  $p_T$  distribution of selected candidates (solid points). The solid histogram represents the result of a fit to the sum of the simulated signal (dashed line) and background (dotted line) contributions.

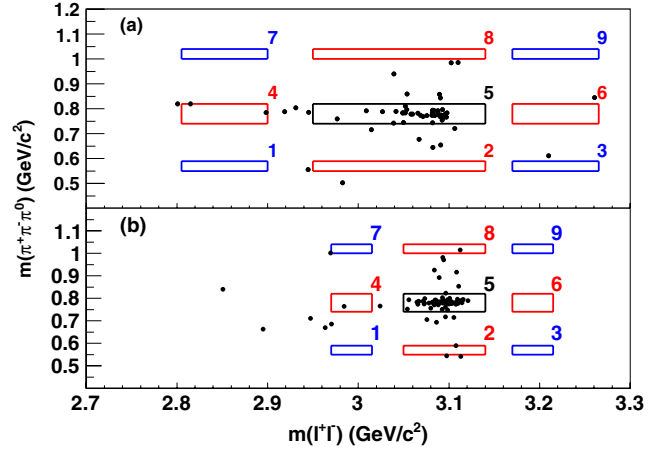


FIG. 2 (color online). Event distribution (solid points) in the  $m(\pi^+ \pi^- \pi^0)$  versus  $m(\ell^+ \ell^-)$  plane for the (a)  $e^+e^-$  and (b)  $\mu^+ \mu^-$  decay mode of the  $J/\psi$ . We also show the  $J/\psi$  signal region (tile 5) and sidebands (tiles 1–4 and 6–9).

a combinatorial background component, modeled using a second-order polynomial function with free parameters. The number of events from combinatorial background in the  $p_T < 0.2 \text{ GeV}/c$  region is  $4 \pm 3$ .

Figure 2 shows the distribution in the  $m(\ell^+ \ell^-) - m(\pi^+ \pi^- \pi^0)$  plane of events that satisfy the selection criteria, except for the  $J/\psi$  and  $\omega$  mass selections. The figure also shows the definitions of signal and background regions, indicated by the tiles labeled 1–9. The signal regions correspond to tile 5. Figures 3(a) and 3(b) show  $m(\ell^+ \ell^-)$  and  $m(\pi^+ \pi^- \pi^0)$  for events in the  $\omega$  and  $J/\psi$  signal regions, respectively. As a consistency check, we assign an  $\omega$ -Dalitz-plot weight [7] to events in the  $J/\psi \omega$  signal region. The procedure makes use of the  $\omega$  decay angular distribution. The helicity angle  $\theta$  is the angle between the  $\pi^+$  and  $\pi^0$  directions in the  $\pi^+ \pi^-$  reference frame. The  $\cos\theta$  distribution is proportional to  $\sin^2\theta$ , and the  $\omega$  signal is projected by giving the  $i$ th event weight

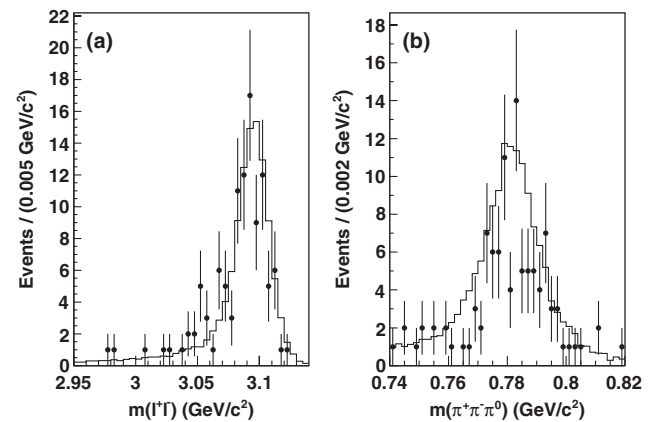


FIG. 3. Data (solid points) and normalized MC (histogram) distributions of (a)  $m(\ell^+ \ell^-)$  for events in the  $\omega$  signal region and (b)  $m(\pi^+ \pi^- \pi^0)$  for events in the  $J/\psi$  signal region.

$w_i = \frac{5}{2}(1 - 3\cos^2\theta_i)$ . The sum of the  $\omega$ -Dalitz-plot weights is consistent with the number of events in the  $J/\psi\omega$  signal region, thus consistent with the hypothesis that most of the observed events do indeed arise from true  $\omega \rightarrow \pi^+\pi^-\pi^0$  decays.

To improve the mass resolution, we define the reconstructed  $J/\psi\omega$  mass as  $m(J/\psi\omega) = m(\ell^+\ell^-\pi^+\pi^-\pi^0) - m(\ell^+\ell^-) + m(J/\psi)^{\text{PDG}}$ . The non- $J/\psi\omega$  background is estimated from the  $J/\psi$  and  $\omega$  sidebands defined in Fig. 2. The  $\omega$  sidebands are defined as  $[0.55, 0.59]$  and  $[1.00, 1.04]$   $\text{GeV}/c^2$ . The  $J/\psi$  sidebands are defined as  $[2.805, 2.900]$  and  $[3.170, 3.265]$   $\text{GeV}/c^2$  for the  $e^+e^-$  channel and  $[2.970, 3.015]$  and  $[3.170, 3.215]$   $\text{GeV}/c^2$  for the  $\mu^+\mu^-$  channel. With these definitions, each sideband size is half of the signal size. The  $m(J/\psi\omega)$  spectrum of this background in the  $J/\psi\omega$  signal region is obtained by  $B(5) = B(2) + B(4) + B(6) + B(8) - (B(1) + B(3) + B(7) + B(9))$ , where  $B(i)$  is the  $m(J/\psi\omega)$  spectrum in the  $i$ th region shown in Fig. 2. The estimated background from this method is  $5 \pm 3$  in good agreement with the estimate from the fit to the  $p_T$  distribution. The residual background from  $\psi(2S) \rightarrow J/\psi\pi^+\pi^-$  decay is estimated by using the values of the integrated luminosity, MC efficiencies, the cross section for  $\psi(2S)$  production in ISR events [20], and the nominal branching fractions for the relevant  $\psi(2S)$  and  $J/\psi$  decays [8]. The expected number of background events from such process is smaller than 0.9 at 90% confidence level (C.L.).

The detection efficiency depends on  $m(J/\psi\omega)$  and  $\theta_\ell^*$ , where  $\theta_\ell^*$  is the angle between the direction of the positively charged lepton from  $J/\psi$  decay ( $\ell^+$ ) and the beam axis in the  $J/\psi\omega$  rest frame. Since we select events in which the  $e^+$  and  $e^-$  beam particles are scattered at small angles, the two-photon axis is approximately the same as the beam axis. Therefore we use the beam axis to determine  $\theta_\ell^*$ .

We parameterize the efficiency dependence with a two-dimensional  $[m(J/\psi\omega), \theta_\ell^*]$  histogram. We label MC events where the reconstructed decay particles are successfully matched to the generated ones as truth-matched events. The detection efficiency in each histogram bin is defined as the ratio between the number of truth-matched MC events that satisfy the selection criteria and the number of MC events that were generated for that bin.

The  $m(J/\psi\omega)$  spectrum is shown in Fig. 4, where each event is weighted to account for detector efficiency, which is almost uniform as a function of the  $J/\psi\omega$  mass. The event weight is equal to  $\bar{\varepsilon}/\varepsilon(m(J/\psi\omega), \theta_\ell^*)$ , where  $\varepsilon(m(J/\psi\omega), \theta_\ell^*)$  is the  $m(J/\psi\omega)$ - and  $\theta_\ell^*$ -dependent efficiency value and  $\bar{\varepsilon}$  is a common scaling factor that ensures all the weights are  $\mathcal{O}(1)$ , since weights far from 1 can cause the estimate of the statistical uncertainty to be incorrect [21]. We observe a prominent peak near 3915  $\text{MeV}/c^2$  over a small background. No evident structure is observed around 3872  $\text{MeV}/c^2$ .

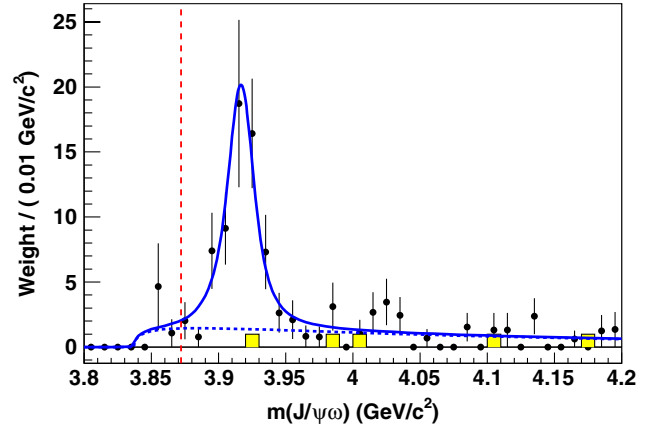


FIG. 4 (color online). The efficiency-corrected  $m(J/\psi\omega)$  distribution of selected events (solid points). The solid line represents the total fit function. The dashed line is the NR contribution. The shaded histogram is the non- $J/\psi\omega$  background defined in the text as  $B(5)$  and estimated from sidebands. The vertical dashed (red) line is placed at  $m(J/\psi\omega) = 3.872$   $\text{GeV}/c^2$ .

We perform an extended unbinned maximum-likelihood fit to the efficiency-corrected  $m(J/\psi\omega)$  spectrum to extract the resonance yield and parameters. In the likelihood function  $\mathcal{L}$  there are two components: one for the  $X(3915)$  signal and one for the nonresonant (NR)  $J/\psi\omega$  contribution. The probability density function (PDF) for the signal component is defined by the convolution of an  $S$ -wave relativistic Breit-Wigner distribution with a detector-resolution function. The NR contribution is taken to be proportional to  $\mathcal{P}_{bg}(m) = p^*(m) \times \exp[-\delta p^*(m)]$ , where  $p^*(m)$  is the  $J/\psi$  momentum in the rest frame of a  $J/\psi\omega$  system with an invariant mass  $m$ ,  $\delta$  is a fit parameter, and  $m = m(J/\psi\omega)$ . The signal and NR yields, the  $X(3915)$  mass and width, and  $\delta$  are free parameters in the fit.

We use truth-matched MC events to determine the signal PDF detector-resolution function. The signal detector-resolution PDF is described by the sum of two Gaussian shapes for the  $X(3915)$  and the sum of a Gaussian plus a Crystal Ball function [22] for the  $X(3872)$ . The parameters of the resolution functions are determined from fits to truth-matched MC events. The widths of the Gaussian core components are 5.7 and 4.5 MeV, respectively, for  $X(3915)$  and  $X(3872)$ . No significant difference in the resolution function parameters is observed for the different  $J/\psi$  decay modes. The parameters of the resolution functions are fixed to their MC values in the maximum-likelihood fit.

The fitted distribution from the maximum-likelihood fit to the efficiency-corrected  $m(J/\psi\omega)$  spectrum is shown in Fig. 4. We observe  $59 \pm 10$  signal events; the measured  $X(3915)$  mass and width are  $(3919.4 \pm 2.2)$   $\text{MeV}/c^2$  and  $(13 \pm 6)$  MeV, respectively, where the uncertainties are statistical only. We add an  $X(3872)$  component, modeled as a  $P$ -wave relativistic Breit-Wigner with mass

3872 MeV/ $c^2$  and width 2 MeV [8], convoluted with the detector-resolution function. No significant change in the result is observed with the addition of this component, whose yield is estimated to be  $1 \pm 4$  events. An excess of events over the fitted NR is observed at  $m(J/\psi \omega) \sim 4025$  MeV/ $c^2$ . If we add a resonant component in the likelihood function to fit this excess, modeled as a Gaussian having free parameters, we obtain a signal yield of  $5 \pm 3$  events.

## V. ANGULAR ANALYSIS OF THE $X(3915)$

We first attempt to discriminate between  $J^P = 0^\pm$  and  $J^P = 2^+$  by using the Rosner [23] predictions. In addition to the previously defined  $\theta_\ell^*$  we consider the following two angles:  $\theta_n^*$  defined as the angle between the normal to the decay plane of the  $\omega(\vec{n})$  and the two-photon axis, and  $\theta_{ln}$  defined as the angle between the lepton  $\ell^+$  from  $J/\psi$  decay and the  $\omega$  decay normal (see Fig. 5). To obtain the normal to the  $\omega$  decay plane we boost the two pions from the  $\omega$  decay into the  $\omega$  rest frame and obtain  $\vec{n}$  by the cross product vector of the two charged pions. A projection of the efficiency values over  $\cos\theta_\ell^*$  in the  $X(3915)$  signal region is shown in Fig. 6(a). The projections of the efficiency over the angles  $\theta_n^*$  and  $\theta_{ln}$  are shown in Figs. 6(b) and 6(c). The efficiency distributions are not uniform and are parameterized by fifth-order polynomials. The  $\cos\theta_\ell^*$ ,  $\cos\theta_n^*$ , and  $\cos\theta_{ln}$  distributions are sensitive to the spin parity of the resonance. We assume that for  $J^P = 2^+$  the dominant amplitude has helicity 2. This is in agreement with previous charmonium measurements [24–26] and theoretical predictions [27,28]. The expected functional forms under this hypothesis are summarized in Table I. Figures 7(a)–7(c) show the efficiency-corrected  $\cos\theta_\ell^*$ ,  $\cos\theta_n^*$ , and  $\cos\theta_{ln}$  distributions for events in the  $X(3915)$  signal region, defined by  $3890 < m(J/\psi \omega) < 3950$  MeV/ $c^2$ . Since the background is small, we assume

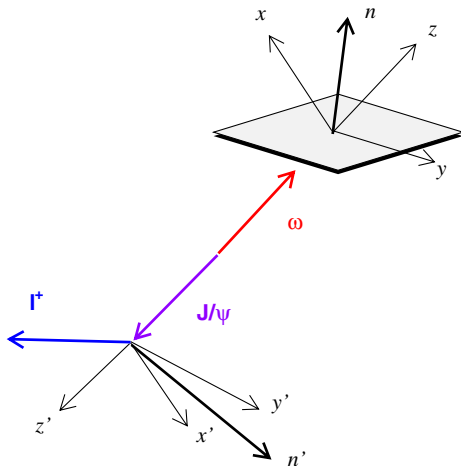


FIG. 5 (color online). Diagram illustrating the reference frames involved in the definition of angular variables.

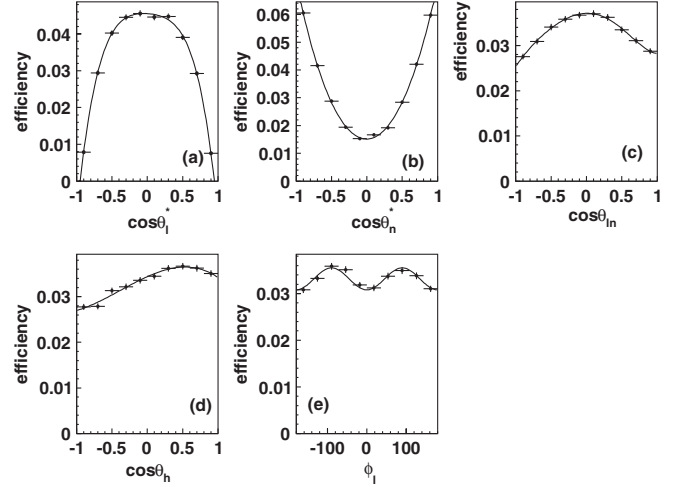


FIG. 6. The efficiency distributions in the  $X(3915)$  signal region  $3890 < m(J/\psi \omega) < 3950$  MeV/ $c^2$  (solid points) as functions of (a)  $\cos\theta_\ell^*$ , (b)  $\cos\theta_n^*$ , (c)  $\cos\theta_{ln}$ , (d)  $\cos\theta_h$ , and (e)  $\phi_l$ . The curves show the results from the fits described in the text.

that all the events come from  $X(3915)$  decay. The distributions for data are compared with the expected curves for  $J^P = 0^\pm$  and  $J^P = 2^+$ . The resulting  $\chi^2$  for each distribution is reported in Table I. In all cases the  $J^P = 0^\pm$  expectations describe the data better than the  $J^P = 2^+$  ones and this is particularly true for the  $\cos\theta_n^*$  distribution. In the latter case  $\chi^2$  probabilities for  $J^P = 0^\pm$  and  $J^P = 2^+$  are, respectively, 64.7% and  $9.6 \times 10^{-9}\%$ . We conclude that the data largely prefer  $J^P = 0^\pm$  over  $J^P = 2^+$ .

The spin-0 hypothesis can be further tested by examining the  $\cos\theta_h$  distribution, where  $\theta_h$  is the angle formed by the  $J/\psi$  momentum in the  $J/\psi \omega$  rest frame with respect to

TABLE I. Functional shapes and  $\chi^2$  for the different spin hypotheses. NDF = 9.

Angle	$J^P = 0^-$	$J^P = 0^+$	$J^P = 0^\pm$	$J^P = 2^+$
$\theta_l^*$			1	$1 + \cos^2\theta_l^*$
$\chi^2$			11.2	16.9
$\theta_n^*$			1	$\sin^2\theta_n^*$
$\chi^2$			6.9	65.9
$\theta_{ln}$			$\sin^2\theta_{ln}$	$7 - \cos^2\theta_{ln}$
$\chi^2$			12.5	18.0
$\theta_h$			1	
$\chi^2$			12.2	
$\theta_n$	$\sin^2\theta_n$	1		
$\chi^2$	77.6	16.3		
$\theta_l$	$1 + \cos^2\theta_l$	1		
$\chi^2$	8.7	8.3		
$\phi_l$	$2 - \cos(2\cos\phi_l)$	$2 + \cos(2\cos\phi_l)$		
$\chi^2$	21.7	9.6		

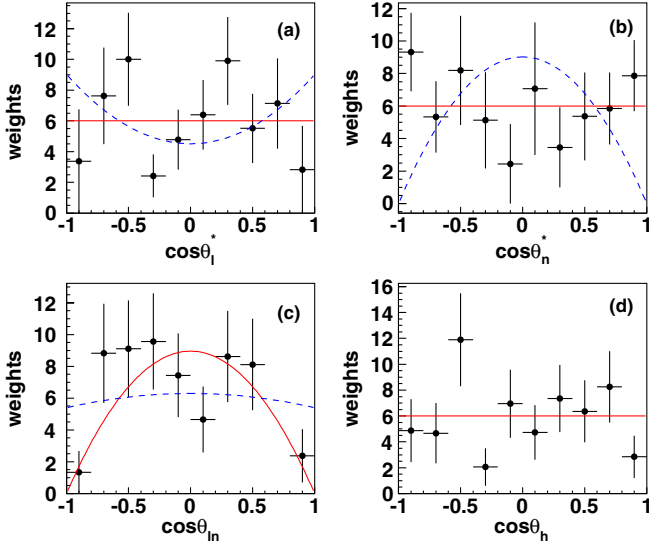


FIG. 7 (color online). The efficiency-corrected distributions of selected events in the  $X(3915)$  signal region  $3890 < m(J/\psi\omega) < 3950 \text{ MeV}/c^2$  (solid points). (a)  $\cos\theta_{\ell^*}$ , (b)  $\cos\theta_n^*$ , (c)  $\cos\theta_{in}$ , and (d)  $\cos\theta_h$ . The solid (red) line represents the expected distribution for the  $J^P = 0^+$  assignment and the dashed (blue) line for the  $J^P = 2^+$ .

the  $J/\psi\omega$  direction in the laboratory frame. The efficiency distribution as a function of  $\cos\theta_h$  is shown in Fig. 6(d), where it is parameterized by a third-order polynomial. The  $\cos\theta_h$  distribution in the  $X(3915)$  signal region, corrected for efficiency, is shown in Fig. 7(d) and is compared with the uniform distribution expected for the spin-0 hypothesis. The resulting  $\chi^2/\text{NDF}$  is 12.2/9 and we conclude that this test also supports the spin-0 assignment.

We attempt to discriminate between  $J^P = 0^-$  and  $J^P = 0^+$ . For this purpose, we define the angles  $\theta_n$ ,  $\theta_l$ , and  $\phi_l$ . To define these angles, we first boost all the 4-vectors into the  $J/\psi\omega$  rest frame. We define  $\theta_n$  to be the angle between the normal to the  $\omega$  decay plane  $\vec{n}$  and the  $\omega$  direction in the  $J/\psi\omega$  rest frame. The efficiency distribution as a function of  $\cos\theta_n$  (not shown) is consistent with being uniform.

For  $J/\psi$  decay, we first boost the  $\ell^+$  to the  $J/\psi$  rest frame. We define  $\theta_l$  as the angle between the  $\ell^+$  and the direction of the  $J/\psi$  in the  $J/\psi\omega$  frame. The efficiency distribution as a function of  $\cos\theta_l$  (not shown) is consistent with being uniform.

Next we define a coordinate system as follows (see Fig. 5). For  $\omega$  decay, we choose the  $z$  axis along the  $\omega$  momentum vector and represent the  $\omega$  decay in terms of its decay plane normal  $\vec{n}$ . The cross product  $\vec{z} \times \vec{n}$  gives the  $y$ -axis direction. Then we define the  $x$ -axis vector by  $\vec{y} \times \vec{z}$ . The  $x-z$  plane, by construction, contains the  $\omega$  decay plane normal.

We now specify the  $J/\psi$  decay coordinate system in terms of the unit vectors defined for  $\omega$  decay. We define  $\vec{z}' = -\vec{z}$ ,  $\vec{x}' = -\vec{x}$ , and  $\vec{y}' = \vec{y}$  so that  $\vec{y}'$  is along the normal

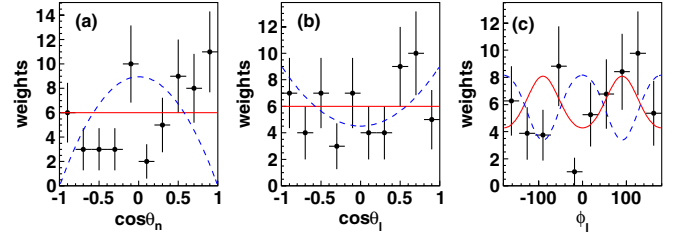


FIG. 8 (color online). The efficiency-corrected distributions of selected events in the  $X(3915)$  signal region  $3890 < m(J/\psi\omega) < 3950 \text{ MeV}/c^2$  (solid points). The (a)  $\cos\theta_n$ , (b)  $\cos\theta_l$ , and (c)  $\phi_l$  distributions are compared with  $J^P = 0^+$  (solid red line) and  $J^P = 0^-$  (dashed blue line) expectations.

to the plane containing the normal to the decay plane of the  $\omega$ . Next we define the  $J/\psi$  decay plane normal  $\vec{n}'$  as the cross product of the  $\ell^+$  in the  $J/\psi$  rest frame and the  $\vec{z}'$  vector. By construction,  $\vec{n}'$  is in the  $x'-y'$  plane. Then we compute the angle  $\phi_l$  as the angle between the  $J/\psi$  and  $\omega$  decay plane normals.

The efficiency distribution as a function of  $\phi_l$  is shown in Fig. 6(e) and is fitted using the function  $\epsilon(\phi_l) = 1 - c \cdot \cos 2\phi_l$ , where  $c$  is a free parameter.

It can be shown that the full angular distribution for  $J^P = 0^-$  can be written as

$$\frac{dN}{d\cos\theta_n d\cos\theta_l d\phi_l} = \frac{9N}{64\pi} \sin^2\theta_n [1 + \cos\theta_l^2 + \sin^2\theta_l \cdot \cos 2\phi_l]. \quad (1)$$

For  $J^P = 0^+$ , assuming no  $D$  wave, the normalized angular distribution is given by

$$\frac{dN}{d\cos\theta_n d\cos\theta_l d\phi_l} = \frac{3N}{32\pi} [2\sin^2\theta_l \cos^2\theta_n + \sin^2\theta_n \cdot (1 + \cos^2\theta_l - \sin^2\theta_l \cos 2\phi_l) + \sin 2\theta_l \cos\phi_l \sin 2\theta_n]. \quad (2)$$

Equations (1) and (2), when projected onto the different angles, give the functional expectations shown in Table I and presented in Fig. 8. The resulting  $\chi^2$  for all the distributions are summarized in Table I. In all cases the  $J^P = 0^+$  hypothesis gives a smaller  $\chi^2$  than the  $J^P = 0^-$  hypothesis and this is particularly true for the  $\cos\theta_n$  distribution. In the latter case  $\chi^2$  probabilities for  $J^P = 0^+$  and  $J^P = 0^-$  are 6.1% and  $4.8 \times 10^{-11}\%$ , respectively. We conclude that the  $J^P = 0^+$  assignment is largely preferred over the  $J^P = 0^-$  assignment.

We observe no correlation between any angles considered in this analysis except for  $\phi_l$  which is strongly correlated with  $\theta_{in}$ .

## VI. SYSTEMATIC UNCERTAINTIES

Several sources contribute to systematic uncertainties on the resonance yields and parameters. Systematic uncertainties due to the functional forms chosen for the PDF

parametrizations and fixed parameters in the fit are estimated to be the sum in quadrature of the changes observed when repeating the fit varying the fixed parameters by  $\pm 1$  standard deviation ( $\sigma$ ). Since the  $X(3915)$  spin assignment is unknown, we repeat the fit by parameterizing the  $X(3915)$  signal as the convolution of a  $P$ -wave relativistic Breit-Wigner with the detector-resolution function. The changes in the fit results are taken as the systematic uncertainty. We examine the dependence of the fit results on the fit range, varying the boundary of the fit from the nominal value of  $4.2 \text{ GeV}/c^2$  (see Fig. 4) to either  $4.1$  or  $4.3 \text{ GeV}/c^2$ . We take as the systematic uncertainty the largest among the observed differences in the fit results. The uncertainty on the absolute mass scale is studied by measuring the difference between the observed and nominal  $J/\psi$  mass in a  $K^+K^-\pi^+\pi^-\pi^0$  ISR-enriched control sample [29]. The  $K^+K^-\pi^+\pi^-\pi^0$  final state has the same number of charged and neutral particles as  $J/\psi$ . The observed difference in mass is  $(-1.1 \pm 0.8) \text{ MeV}/c^2$ . We take the sum in quadrature of this shift with its uncertainty as a systematic uncertainty. Previous studies show that MC events have a better mass resolution than data [29]. The effect of possible differences between data and MC in the  $m(J/\psi \omega)$  resolution is estimated by increasing the width of the resolution function core component by 20%. The uncertainty due to the use of efficiency weights to correct the  $m(J/\psi \omega)$  spectrum is estimated with simulated experiments. In each experiment, we randomly modify the efficiency weight according to its statistical uncertainty. We then fit the resulting mass spectra and plot the resulting yields and resonance parameters. The resulting spreads give the systematic uncertainties on these quantities. We find that the fit bias on the yield is negligible.

The  $X(3915)$  signal significance is  $7.6\sigma$ , calculated from  $-2 \ln(\mathcal{L}_0/\mathcal{L}_{\text{max}})$ , where  $\mathcal{L}_0$  and  $\mathcal{L}$  are the likelihoods of the fits with and without the resonant component, respectively. The difference in the number of degrees of freedom is taken into account. Systematic uncertainties are incorporated into the likelihood function by convolving it with a Gaussian with mean equal to zero and width equal to the systematic uncertainty on the yield.

The product between the two-photon coupling  $\Gamma_{\gamma\gamma}$  and the resonance branching fraction  $\mathcal{B}$  to the  $J/\psi \omega$  final state is measured using  $473.8 \text{ fb}^{-1}$  of data collected near the  $Y(4S)$  energy. The efficiency-weighted yields for the resonances, the integrated luminosity near the  $Y(4S)$  energy, and the branching fractions  $\mathcal{B}(J/\psi \rightarrow \ell^+\ell^-) = (5.94 \pm 0.06)\%$  [8] and  $\mathcal{B}(\omega \rightarrow \pi^+\pi^-\pi^0) = (89.2 \pm 0.7)\%$  [8] are used to obtain  $\Gamma_{\gamma\gamma} \times \mathcal{B}$  using the GamGam generator. In this calculation, the  $X(3915)$  parameters are fixed to the values obtained from the fit.

The uncertainties on the weighted signal yield described above are taken into account in the  $\Gamma_{\gamma\gamma} \times \mathcal{B}$  systematic error. Systematic uncertainties on the efficiency due to

tracking (0.3% per track),  $\pi^0$  reconstruction (3.0%) and particle identification (0.1% per pion, 0.8% per lepton) are obtained from auxiliary studies. The uncertainty on the luminosity is 1.1%. The uncertainty on the nominal  $J/\psi$  and  $\omega$  branching fractions used in the calculation is propagated in the  $\Gamma_{\gamma\gamma} \times \mathcal{B}$  error. The GamGam calculation has an uncertainty of 3% [3].

Since no significant  $X(3872)$  signal is observed, we determine a Bayesian upper limit (UL) at 90% C.L. on  $\Gamma_{\gamma\gamma} \times \mathcal{B}$ , assuming a uniform prior probability distribution. The upper limit for  $\Gamma_{\gamma\gamma} \times \mathcal{B}$  is thus computed according to

$$\int_0^{\text{UL}} L(\Gamma_{\gamma\gamma} \times \mathcal{B}) d(\Gamma_{\gamma\gamma} \times \mathcal{B}) = 0.90,$$

where  $L(\Gamma_{\gamma\gamma} \times \mathcal{B})$  is the likelihood function for  $\Gamma_{\gamma\gamma} \times \mathcal{B}$ .

For a  $J=0$  resonance, the resulting value of  $\Gamma_{\gamma\gamma}[X(3915)] \times \mathcal{B}(X(3915) \rightarrow J/\psi \omega)$  is  $(52 \pm 10 \pm 3) \text{ eV}$  where the first uncertainty is statistical and the second systematic. For completeness we also report the value for  $J=2$ :  $(10.5 \pm 1.9 \pm 0.6) \text{ eV}$ . For  $X(3872)$ , we obtain  $\Gamma_{\gamma\gamma}[X(3872)] \times \mathcal{B}(X(3872) \rightarrow J/\psi \omega) < 1.7 \text{ eV}$  at 90% C.L., assuming  $J=2$ .

## VII. SUMMARY

In summary, we confirm the observation of the charmoniumlike resonance  $X(3915)$  in the  $\gamma\gamma \rightarrow J/\psi \omega$  process, with a significance of  $7.6\sigma$ , including systematic uncertainties. The measured mass and width are

$$m[X(3915)] = (3919.4 \pm 2.2 \pm 1.6) \text{ MeV}/c^2,$$

$$\Gamma[X(3915)] = (13 \pm 6 \pm 3) \text{ MeV},$$

where the first uncertainty is statistical and the second systematic. These measurements are consistent with those previously reported by Belle for the same process [6] and by *BABAR* [5] and Belle [4] for  $B \rightarrow J/\psi \omega K$ . A detailed angular analysis has been performed. We find that the data largely prefer  $J^P = 0^\pm$  over  $J^P = 2^+$ . In this hypothesis,  $J^P = 0^+$  is largely preferred over  $J^P = 0^-$  and this would identify the signal as being due to the  $\chi_{c0}(2P)$  resonance. The mass of  $X(3915)$  is consistent with the result of the potential model, which predicts the mass of the first radial excitation  $\chi_{c0}$  to be around  $3916 \text{ MeV}$  according to the Godfrey-Isgur relativized potential model [30]. The product  $\Gamma_{\gamma\gamma}[X(3915)] \times \mathcal{B}[X(3915) \rightarrow J/\psi \omega]$  is also measured. The value for  $J=0$  (relatively large compared to charmonium model predictions) is consistent with that reported by Belle [6]. This product, also computed in this analysis for  $J=2$ , is smaller than the corresponding value obtained by Belle. We have also searched for the  $\gamma\gamma \rightarrow X(3872) \rightarrow J/\psi \omega$  process, but no significant signal is found.

## ACKNOWLEDGMENTS

We are grateful for the extraordinary contributions of our PEP-II colleagues in achieving the excellent luminosity and machine conditions that have made this work possible. The success of this project also relies critically on the expertise and dedication of the computing organizations that support *BABAR*. The collaborating institutions wish to thank SLAC for its support and the kind hospitality extended to them. This work is supported by the U.S. Department of Energy and National Science Foundation, the Natural Sciences and Engineering Research Council (Canada), the Commissariat à l'Énergie Atomique and Institut National de Physique

Nucléaire et de Physique des Particules (France), the Bundesministerium für Bildung und Forschung and Deutsche Forschungsgemeinschaft (Germany), the Istituto Nazionale di Fisica Nucleare (Italy), the Foundation for Fundamental Research on Matter (Netherlands), the Research Council of Norway, the Ministry of Education and Science of the Russian Federation, Ministerio de Ciencia e Innovación (Spain), and the Science and Technology Facilities Council (United Kingdom). Individuals have received support from the Marie-Curie IEF program (European Union), the A. P. Sloan Foundation (USA) and the Binational Science Foundation (USA–Israel).

- 
- [1] B. Aubert *et al.* (*BABAR* Collaboration), *Phys. Rev. Lett.* **95**, 142001 (2005); T.E. Coan *et al.* (CLEO Collaboration), *Phys. Rev. Lett.* **96**, 162003 (2006); C.Z. Yuan *et al.* (Belle Collaboration), *Phys. Rev. Lett.* **99**, 182004 (2007); B. Aubert *et al.* (*BABAR* Collaboration), *Phys. Rev. Lett.* **98**, 212001 (2007); X.L. Wang *et al.* (Belle Collaboration), *Phys. Rev. Lett.* **99**, 142002 (2007).
- [2] S. Uehara *et al.* (Belle Collaboration), *Phys. Rev. Lett.* **96**, 082003 (2006).
- [3] B. Aubert *et al.* (*BABAR* Collaboration), *Phys. Rev. D* **81**, 092003 (2010).
- [4] S.-K. Choi *et al.* (Belle Collaboration), *Phys. Rev. Lett.* **94**, 182002 (2005).
- [5] B. Aubert *et al.* (*BABAR* Collaboration), *Phys. Rev. Lett.* **101**, 082001 (2008).
- [6] S. Uehara *et al.* (Belle Collaboration), *Phys. Rev. Lett.* **104**, 092001 (2010).
- [7] P. del Amo Sanchez *et al.* (*BABAR* Collaboration), *Phys. Rev. D* **82**, 011101(R) (2010).
- [8] K. Nakamura *et al.* (Particle Data Group), *J. Phys. G* **37**, 075021 (2010).
- [9] X. Liu, Z.-G. Luo, and Z.-F. Sun, *Phys. Rev. Lett.* **104**, 122001 (2010).
- [10] T. Branz, R. Molina, and E. Oset, *Phys. Rev. D* **83**, 114015 (2011).
- [11] X. Liu, Z.-G. Luo, Y.-R. Liu, and S.-L. Zhu, *Eur. Phys. J. C* **61**, 411 (2009); T. Branz, T. Gutsche, and V. Lyubovitskij, *Phys. Rev. D* **80**, 054019 (2009); W.H. Liang, R. Molina, and E. Oset, *Eur. Phys. J. A* **44**, 479 (2010).
- [12] S.-K. Choi *et al.* (Belle Collaboration), *Phys. Rev. Lett.* **91**, 262001 (2003).
- [13] N. Brambilla *et al.*, *Eur. Phys. J. C* **71**, 1534 (2011).
- [14] B. Aubert *et al.* (*BABAR* Collaboration), *Phys. Rev. Lett.* **102**, 132001 (2009); V. Bhardwaj *et al.* (Belle Collaboration), *Phys. Rev. Lett.* **107**, 091803 (2011).
- [15] A. Abulencia *et al.* (CDF Collaboration), *Phys. Rev. Lett.* **98**, 132002 (2007).
- [16] S.-K. Choi *et al.* (Belle Collaboration), *Phys. Rev. D* **84**, 052004 (2011).
- [17] C.N. Yang, *Phys. Rev.* **77**, 242 (1950).
- [18] B. Aubert *et al.* (*BABAR* Collaboration), *Nucl. Instrum. Methods Phys. Res., Sect. A* **479**, 1 (2002).
- [19] The *BABAR* detector Monte Carlo simulation is based on GEANT4 [S. Agostinelli *et al.*, *Nucl. Instrum. Methods Phys. Res., Sect. A* **506**, 250 (2003)] and EVTGEN [D.J. Lange, *Nucl. Instrum. Methods Phys. Res., Sect. A* **462**, 152 (2001)].
- [20] J.P. Alexander *et al.*, Report No. SLAC-PUB-4501, 1998; M. Benayoun, S.I. Eidelman, V.N. Ivanchenko, and Z.K. Silagadze, *Mod. Phys. Lett. A* **14**, 2605 (1999).
- [21] A.G. Frodesen *et al.*, *Probability and Statistics in Particle Physics* (Universitetsforlaget, Bergen, Norway, 1979).
- [22] M.J. Oreglia, Ph.D. thesis, Stanford Report No. SLAC-236, 1980, Appendix D; J.E. Gaiser, Ph.D. thesis, Stanford Report No. SLAC-255, 1982, Appendix F; T. Skwarnicki, Ph.D. thesis, DESY Report No. DESY F31-86-02, 1986, Appendix E.
- [23] J.L. Rosner, *Phys. Rev. D* **70**, 094023 (2004).
- [24] S. Uehara *et al.* (Belle Collaboration), *Phys. Rev. D* **78**, 052004 (2008).
- [25] B. Aubert *et al.* (*BABAR* Collaboration), *Phys. Rev. D* **81**, 092003 (2010).
- [26] M. Ablikim *et al.* (BESIII Collaboration), *Phys. Rev. D* **85**, 112008 (2012).
- [27] M. Poppe, *Int. J. Mod. Phys. A* **1**, 545 (1986).
- [28] G.A. Schuler, F.A. Berends, and R. van Gulik, *Nucl. Phys.* **B523**, 423 (1998).
- [29] P. del Amo Sanchez *et al.* (*BABAR* Collaboration), *Phys. Rev. D* **84**, 012004 (2011).
- [30] T. Barnes, S. Godfrey, and E. S. Swanson, *Phys. Rev. D* **72**, 054026 (2005).